Properties of Slo1 K$^+$ channels with and without the gating ring

Gonzalo Budelli[a], Yanyan Geng[b], Alice Butler[a], Karl L. Magleby[b], and Lawrence Salkoff[a,c,1]

Departments of [a]Anatomy and Neurobiology and [c]Genetics, Washington University School of Medicine in St. Louis, St. Louis, MO 63110; and [b]Department of Physiology and Biophysics, University of Miami Miller School of Medicine, Miami, FL 33136

High-conductance Ca^{2+}- and voltage-activated K$^+$ (Slo1 or BK) channels (*KCNMA1*) play key roles in many physiological processes. The structure of the Slo1 channel has two functional domains, a core consisting of four voltage sensors controlling an ion-conducting pore, and a larger tail that forms an intracellular gating ring thought to confer Ca^{2+} and Mg^{2+} sensitivity as well as sensitivity to a host of other intracellular factors. Although the modular structure of the Slo1 channel is known, the functional properties of the core and the allosteric interactions between core and tail are poorly understood because it has not been possible to study the core in the absence of the gating ring. To address these questions, we developed constructs that allow functional cores of Slo1 channels to be expressed by replacing the 827-amino acid gating ring with short tails of either 74 or 11 amino acids. Recorded currents from these constructs reveals that the gating ring is not required for either expression or gating of the core. Voltage activation is retained after the gating ring is replaced, but all Ca^{2+}- and Mg^{2+}-dependent gating is lost. Replacing the gating ring also right-shifts the conductance-voltage relation, decreases mean open-channel and burst duration by about sixfold, and reduces apparent mean single-channel conductance by about 30%. These results show that the gating ring is not required for voltage activation but is required for Ca^{2+} and Mg^{2+} activation. They also suggest possible actions of the unliganded (passive) gating ring or added short tails on the core.

BK channel | iberiotoxin | tetraethylammonium | β1 subunit | Kv1.4

Slo1 channels are expressed in most human tissues and play key roles in many important physiological processes, including smooth muscle contraction, neurotransmitter release, neuronal excitability, hair cell tuning, and action potential termination (1–6). Slo1 channels also are named BK (Big K$^+$) or MaxiK channels because of their high single-channel conductance (~300 pS in 150-mM symmetrical K$^+$). Slo1 channels are activated synergistically by both depolarization and intracellular calcium (7–9), linking these two activators in a negative feedback system to restore negative membrane potential which, in turn, closes voltage-activated Ca^{2+} channels. The dual regulation by voltage and calcium led Hille (10) to predict that BK channels function like the classical Hodgkin–Huxley delayed rectifier channel, except that the range of voltage activation was set by the intracellular Ca^{2+} concentration. The cloning (11) and analysis of the Slo1 channel structure seemed to validate this prediction, in that Slo1 appeared to be modular in its construction, having a core domain containing a voltage sensor controlling a K$^+$-selective pore and a long C-terminal tail forming a gating ring structure comprised of four pairs of regulators of the conductance of K$^+$ (RCK) domains for sensing and transducing the effect of Ca^{2+} binding to the core.

One of the four identical α subunits that assemble to form the Slo1 WT channel (Slo1-WT) is shown in Fig. 1 *Top*. For the mbr5 cDNA (12) used in this study, the "core" consists of 342 residues including seven transmembrane segments (S0–S6) and the S6–RCK1 linker sequence, which is attached to a long tail of 827 residues. The tail sequence of Slo1-WT is distinct from the cytoplasmic domains of other members of the K$^+$ channel extended

family. Structure–function studies of the tail have shown the existence of two high-affinity Ca^{2+} binding sites (13, 14) and one low-affinity Mg^{2+} site (14, 15). Modulation of the channel also occurs by additional biological factors, including protons, heme, carbon monoxide, phosphorylation, and oxidation (16–20), all of which may function via their interaction with the tail. Thus, the large tail accommodates a variety of regulatory domains which sense different intracellular factors, leading to pushing or tugging against the core to facilitate or inhibit channel gating. These complicated allosteric interactions between core and tail almost certainly involve several transduction pathways (21–23), all of which alter the properties of the core. Thus, a logical starting point to begin investigating the allosteric interactions would be to understand the baseline properties of the isolated core. However, this approach has been hampered by the inability to express functional cores in the absence of the tail. Previous analysis of truncated expression constructs of Slo1 channels found that their processing stalls in the endoplasmic reticulum (ER), they are not assembled into tetramers, they fail to be exported to the plasma membrane, or they are nonfunctional (24). We now show that core constructs without gating rings can be expressed by leaving a short region required for subunit tetramerization and by appending a small tail domain which facilitates processing and efficient export to the plasma membrane. Thus, we now are able to investigate gating in the absence of a gating ring.

Results

Slo1 Core Constructs Express Currents. The constructs we have synthesized to achieve autonomous expression of the Slo1 core are shown in Fig. 1. The top diagram in Fig. 1 shows the schematic structure of the WT Slo1 BK channel subunit (Slo1-WT),

---

Significance

High-conductance Slo1 (BK) K$^+$ channels are synergistically activated by Ca^{2+}, voltage, Mg^{2+}, and additional factors to modulate membrane excitability in many key physiological processes. Slo1 channels are of modular design with allosteric interactions between the core transmembrane modules and a large cytoplasmic gating ring module, providing a model system to study allosteric principles in channel gating and protein function. To examine the allosteric interactions, we developed constructs that replace the large gating ring module with short peptides and then characterized the altered properties of the gating. Our studies, which provide insight into functional and allosteric interactions between the core and the gating ring, may be useful in understanding the disease processes associated with Slo1-channel dysfunction.
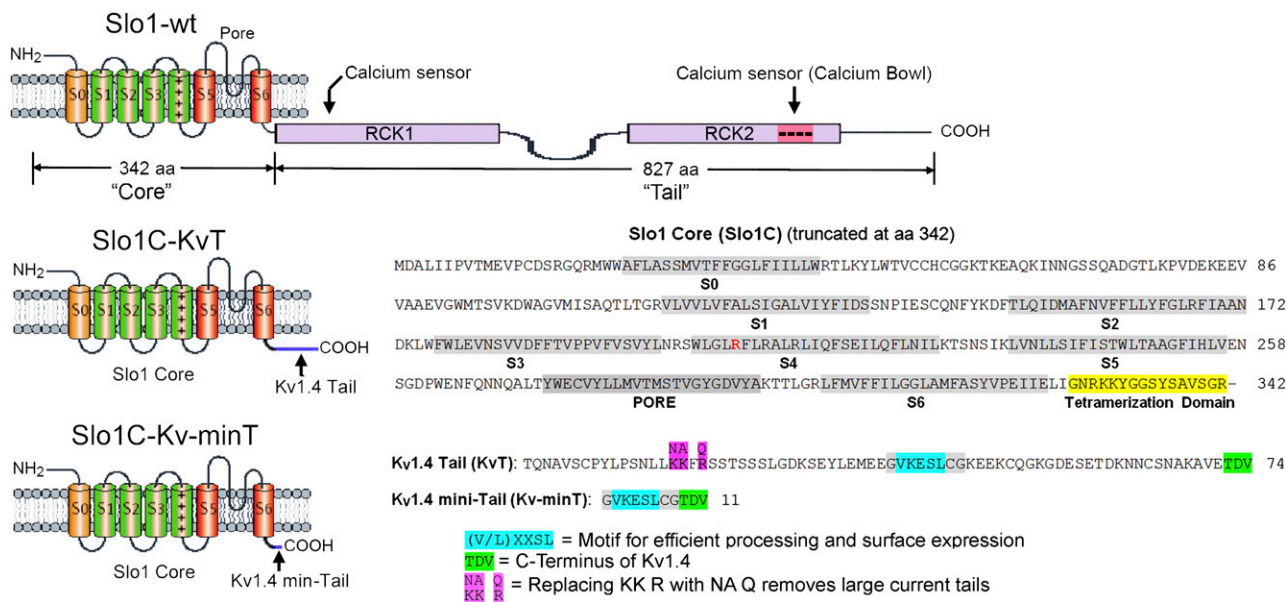

Fig. 1. Slo1 channel constructs used in this study. The Slo1 channel constructs used in this study are based on the mouse mbr5 cDNA (12) and the mouse Shaker family Kv1.4 channel (25). The "Slo1 core and tail" refers to the first 342 and the last 827 amino acid residues. The "Kv1.4 tail" refers to the last 74 amino acid residues of Kv1.4. The different channel constructs are designated as follows: Slo1-WT is Slo1 full-length WT; Slo1C-KvT is a Slo1 core with a 74-residue Kv1.4 tail; Slo1C-Kv-minT is a Slo1 core with a Kv1.4 11-residue mini tail; Slo1C-KvT$_{NAFQ}$ is a Slo1 core with a 74-residue Kv1.4 tail with NAFQ substituted for KKFR in the tail; Slo1C-KvT R207E is Slo1C-KvT with R207E in S4 in the core.

which has seven transmembrane segments containing a voltage sensor and a K$^+$-selective pore (labeled "core") and a larger cytoplasmic region containing two tandem regulators of K$^+$ conductance (RCK1 and RCK2), each with a Ca^{2+} sensor (labeled "tail"). Two impediments to the functional expression of truncated core constructs are their entrapment within the ER and their failure to form tetramers (24). We addressed the first of these problems by creating a construct (Slo1C-KvT) which contained a 74-amino acid C-terminal region (labeled Kv1.4 tail in Fig. 1) from the Kv1.4 voltage-sensitive K$^+$ channel which contains a conserved motif (Fig. 1, highlighted in blue) reported to facilitate the efficiency of channel expression and export to the plasma membrane (25). This added region is less than 10% the size of the normal Slo1-WT tail domain (Fig. 1). The second problem was addressed by including the last 16 residues of the core which extend into the cytoplasm from the base of S6 (Fig. 1,

highlighted in yellow). This region was reported to be important to the formation of channel tetramers (24, 26).

Amazingly, this channel construct expressed currents, and the magnitudes of the expressed currents for both whole-cell recording and inside-out patches were as large as those achieved by the expression of WT channels (Fig. 2 A and B; Slo1C-KvT). Curiously, however, large, slowly decaying tail currents were present in these current records (arrows) which were not seen in Slo1-WT channels. These tail currents reversed at the K$^+$ equilibrium potential, indicating that the currents are the product of a K$^+$-selective channel. To examine whether these tail currents might be a property resulting from a motif present in the added 74-residue Kv1.4 C-terminal region, we made a second construct that includes only 11 residues of the Kv1.4 C-terminal sequence: the five residues reported to be essential for surface expression (Fig. 1, highlighted in blue) (25) and the last three residues of the Kv1.4 terminal sequence (Fig. 1, highlighted in green). Large
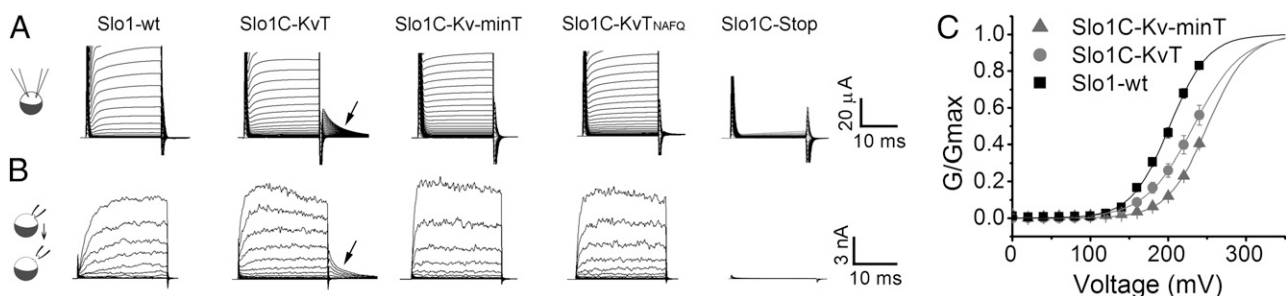

Fig. 2. Slo1 constructs without gating rings express large currents in *Xenopus* oocytes. (A) Whole-cell current recordings from oocytes injected with cRNAs of the indicated constructs (see Fig. 1 and legend). Currents were not observed when a stop codon was placed immediately after the tetramerization domain at position 342 (Slo1C-Stop). With a two-electrode voltage clamp, oocytes were held at −70 mV, and 20-ms step pulses were applied from −70 mV to 250 mV in 10-mV increments followed by a step to 0 mV to see outward tail currents in an ND96 bath solution. Not all traces are shown. (B) Currents recorded from inside-out macropatches from oocytes injected with the constructs in A. Asymmetric K$^+$ with 10 mM K$^+$ in pipette and 140 mM K$^+$ on the inside of membrane was used. A 50-ms prepulse to −100 mV was followed by 20-ms step pulses from −100 to 240 mV in 20-mV increments followed by a step to 0 mV for 10 ms. Arrows indicate prominent tail currents observed for Slo1C-KvT. (C) The G–V curve for Slo1-WT is left-shifted compared with Slo1C-KvT and Slo1C-Kv-minT. Data were obtained from Inside-out macropatch recordings in symmetrical 140 mM K$^+$.

macroscopic currents also were expressed by this Slo1C-Kv-minT construct, but the expressed currents lacked the prominent tail currents seen when the full-length Kv1.4 terminal sequence was present (Fig. 2 *A* and *B*, Slo1C-Kv-minT). We also observed that during voltage steps Slo1C-KvT currents typically had a greater time-dependent decrease in amplitude than Slo1C-Kv-minT currents.

One possible interpretation of these results is that the added 74-residue Kv1.4 tail blocks the channel and then is expelled upon repolarization, thus producing the prominent tail currents seen in Fig. 2 *A* and *B* (arrows), perhaps similar to peptide blocking of Shaker channels (27). To test the involvement of the Kv1.4 tail, we neutralized three positively charged residues grouped in the Kv1.4 tail (Fig. 1, highlighted in magenta). Expression of this construct (Fig. 2 *A* and *B*, Slo1C-KvT$_{NAFQ}$) eliminated the prominent tail currents in Slo1C-KvT channels and produced currents virtually indistinguishable from the Slo1C-Kv-minT construct.

The Recorded Currents Are Not from Endogenous Channels. Our ability to change the properties of the expressed currents by modifying the primary structure of the Kv1.4 sequences added to the C terminus of the Slo1 core provided evidence that the observed currents were from channels encoded by the cRNA injected into *Xenopus* oocytes. As an additional control, we created a cDNA identical to the Slo1C constructs except that all the Kv1.4 sequence was omitted and a Stop codon was added immediately following the 16-residue tetramerization domain (Fig. 1, highlighted in yellow). Injection of cRNA from this construct into *Xenopus* oocytes failed to produce any detectable currents (Fig. 2 *A* and *B*, Slo1C-Stop). In a further test to verify that the recorded currents resulted from the expression of the constructs without gating rings, we altered the voltage sensor of the Slo1C-KvT channel (R207E) and observed that the conductance-voltage (G-V) curve shifted to the left and decreased its slope (Fig. 3), consistent with results reported for the same mutation in Slo1-WT channels (28, 29). Having demonstrated that we can express functional Slo1 channels after replacing their gating ring with short 11- and 74-residue tails, we next examined the properties of these constructs.

Voltage Sensitivity Is Retained and the Voltage for Half Activation Is Right-Shifted for Slo1C-KvT and Slo1C-Kv-minT Channels. The retention of voltage-dependent gating in Slo1 channels without gating rings might be expected because the voltage sensor (S1–S4) is contained in the core of the channel (Fig. 1). Indeed, as shown in Figs. 2 and 3, the manipulation of the voltage-dependent gating of the Slo1C-KvT and Slo1C-Kv-minT channels through mutation helped establish that the observed currents were the products of the expressed constructs. The voltage sensitivity of Slo1C-KvT and Slo1C-Kv-minT channels was found to be similar to that of Slo1-WT channels (comparable slopes), but with the voltage for half activation ($V_{1/2}$) right-shifted 27.8 ± 5.8 mV for Slo1C-KvT and 49.2 ± 3.0 mV for Slo1C-Kv-minT relative to Slo1-WT (Fig. 2C). These significant right-shifts ($P < 0.001$, $n \geq 5$) indicate that replacing the unliganded Slo1 gating ring with the KvT or Kv-minT sequences allosterically alters the voltage range of activation. The change in activation to more positive voltages could arise from a possible lack of pull on S6 through the RCK1–S6 linkers because of the absence of the gating ring (see ref. 21) or from the short tails inhibiting open probability (Po) in some manner. In either case, these observations indicate that direct allosteric input from the gating ring to the core is not required for voltage-dependent channel activation.

The Gating Ring Is Required for Ca^{2+} and Mg^{2+} Sensitivity of Slo1 Channels. Structure–function studies have suggested that Ca^{2+} and Mg^{2+} activation of Slo1 channels works through the gating
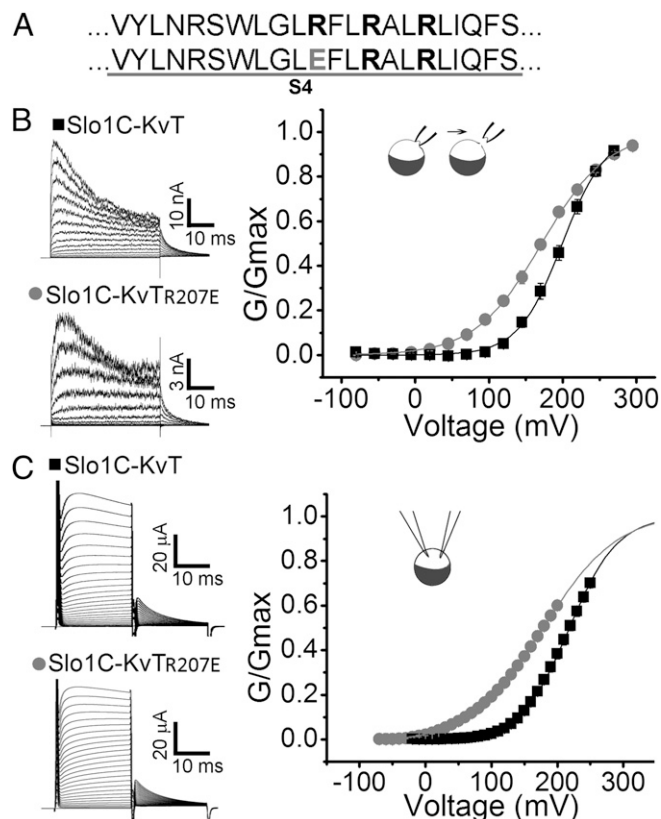

Fig. 3. Verification that the Slo1C-KvT construct without a gating ring is expressed and functional. The R207E mutation in S4 in the voltage sensor of Slo1-KvT left-shifted the voltage-dependent activation of Slo1C-KvT as expected from previous Slo1-WT experiments (22, 23), indicating that the isolated core of Slo1 channels without gating rings is being expressed. (*A*) Sequence of S4 (*Upper*) in the voltage sensor of Slo1 and with the R207E mutation (*Lower*). (*B*) Currents from inside-out macropatches from oocytes injected with Slo1C-KvT and Slo1C-KvT-R207E. G–V plots ($n = 5$) are shown on the right. The voltage protocol was −80 mV for 20 ms followed by a 40-ms voltage step of −80 to +295 mV (in 25-mV increments), followed by steps to 0 mV for 20 ms to measure tail currents. Asymmetric K$^+$ with 10 K$^+$ in pipette and 150 K$^+$ at intracellular side was used. (*C*) Whole-cell currents recorded from Slo1C-KvT and Slo1C-KvT-R207E channels. Oocytes were held at −70 mV and 20-ms step pulses applied from −90 mV to 240 mV with a step back to 0 mV. G–V plots are shown on the right. Solutions are as in Fig. 2 for whole-cell recording.

ring (13–16, 21, 30, 31). We now test this suggestion directly by examining Ca^{2+} and Mg^{2+} sensitivity in Slo1 channels in which the gating ring has been replaced by the KvT or Kv-minT sequences using three different experimental approaches. In all cases, no significant sensitivity to Ca^{2+} or Mg^{2+} was observed. Single-channel recordings showed that exposing inside-out patches to 100 μM Ca^{2+} or 10 mM Mg^{2+} greatly increased Po in Slo1-WT channels by 530 ± 110- or 53 ± 12-fold, respectively, compared with negligible effects on SloC-Kv-minT channels (Fig. 4 *A* and *B*, Fig. S1, and Table S1). When voltage ramps were applied to inside-out patches expressing Slo1-WT, Slo1C-KvT, or Slo1C-Kv-minT channels, channel activity increased as the membrane potential was made more positive for all three channel types (Fig. 4C *Top*). Application of 200 μM Ca^{2+} or 10 mM Mg^{2+} greatly increased channel activity for Slo1-WT channels but had no apparent effect on Slo1C-KvT or Slo1C-Kv-minT channels (Fig. 4C; note calibration bars). A similar result was observed when G–V relationships were obtained in the absence and presence of intracellular Ca^{2+} and Mg^{2+}; the $V_{1/2}$ for Slo1-WT channels was left-shifted toward more negative potentials by 228 ± 5.5 mV
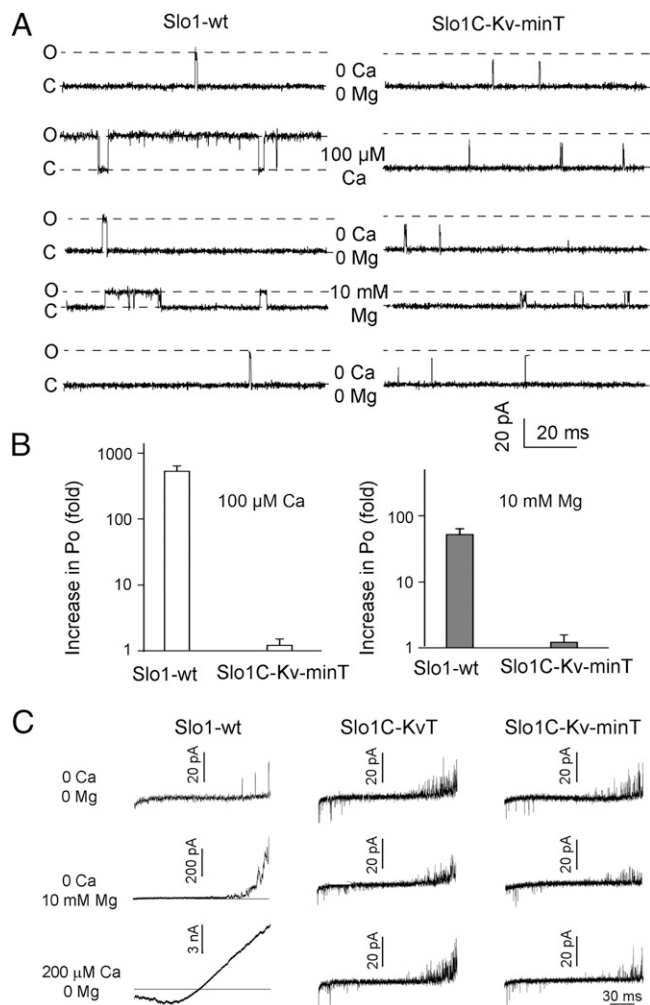
Slo1C-Kv-minT channels compared with Slo1-WT channels ($P < 0.02$, $n \geq 3$) (Fig. 6 and Table S2). These marked changes in single-channel kinetics show that replacing the unliganded gating ring in Slo1 channels with the Kv-minT sequence has profound effects on channel gating. Whether these properties represent the true baseline properties of the core in isolation from allosteric input from the gating ring or whether the Kv-minT peptide is a contributing factor remains to be determined.

The Apparent Mean Single-Channel Conductance Is Reduced for Slo1C-Kv-minT Channels. The high conductance of Slo1-WT channels compared with other K^+-selective channels is one of the defining properties of Slo1-WT channels (10). Unexpectedly, we found that replacing the gating ring with the KV-minT construct decreased single-channel current amplitudes (Figs. 4A and 6), suggesting an apparent decreased conductance. When measurements of currents were restricted to openings of sufficient duration so that their amplitudes should not be attenuated by the low-pass filtering, replacing the gating ring decreased apparent mean single-channel conductance by ~30%, from 307 ± 7 pS for Slo1-WT channels to 213 ± 6 pS for Slo1C-Kv-minT channels ($P < 0.001$, $n = 3$ patches, in each case with mean conductance for each patch determined
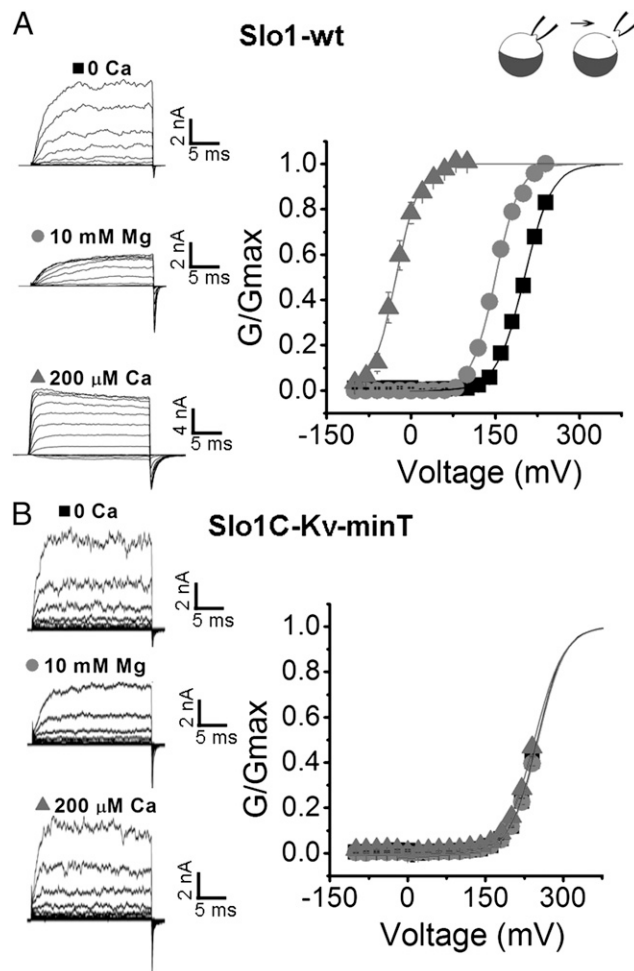
Fig. 4. The gating ring is required for activation by Ca^{2+} and Mg^{2+}. (A) Representative single-channel current activity from Slo1-WT and Slo1C-Kv-minT. Inside-out patches were held at +80 mV, and the intracellular side of membrane was exposed to Ca^{2+} or Mg^{2+} in the sequence indicated. Symmetrical 150 mM K^+ was used. Open (O) and closed (C) current levels are indicated. Ca^{2+} (100 μM) or (10 mM Mg^{2+}) activates Slo1-WT channels but has little effect on Slo1C-Kv-minT channels. Mg^{2+} (10 mM) decreased single-channel conductance (47) for both Slo1-WT and Slo1C-Kv-minT. (B) Ca^{2+} and Mg^{2+} significantly increase Po in Slo1-WT channels ($P < 0.0001$, $n = 5$ for Ca^{2+} and $P < 0.05$, $n = 6$ for Mg^{2+}, paired t tests before normalization) but have insignificant effects on Slo1C-Kv-minT channels ($P > 0.1$, $n = 4$ in each case). Note log scale on ordinate. (C) Current traces from inside-out patches ramped from −90mV to 90 mV in the absence and presence of Ca^{2+} or Mg^{2+} as indicated. Slo1C-KvT and Slo1C-Kv-MinT currents are not detectably activated by 200 μM Ca^{2+} or 10 mM Mg^{2+}. Note differences in scale bars for Slo1-WT. Increasing single-channel activity in the ramps at positive voltages indicates voltage sensitivity in all channel constructs. Symmetrical 140 K^+ was used.

with 200 μM Ca^{2+} and by 51.2 ± 1.9 mV with 10 mM Mg^{2+} (Fig. 5A). In contrast, the $V_{1/2}$ of Slo1C-Kv-minT was not shifted by Ca^{2+} or Mg^{2+} (Fig. 5B), and normalized I–V curves for Slo1C-KvT channels were not shifted when exposed to 200 μM Ca^{2+} (Fig. S2). Hence, the gating ring is required for Ca^{2+} and Mg^{2+} sensitivity of Slo1 channels.

Mean Channel Open Time and Burst Duration Are Greatly Reduced for Slo1C-Kv-minT Channels. The single-channel kinetics of Slo1C-Kv-minT channels differed markedly from those of the Slo1-WT channels. Mean open-interval duration and mean burst duration were decreased significantly, by 5.5- and 6.3-fold, respectively, for

Fig. 5. The gating ring is required for Ca^{2+} and Mg^{2+} to left-shift the G–V curves. (A and B) Currents recorded from inside-out macropatches from Slo1-WT channels (A) or from Slo1C-Kv-minT channels (B) with the G–V curves plotted to the right. The potential was held at 0 mV, stepped to −100 mV for 50 ms, and then stepped from −100 mV to 240 mV in 20-mV increments followed by a step to −80 mV to measure tail currents (Left). Symmetrical 140 K^+ was used.
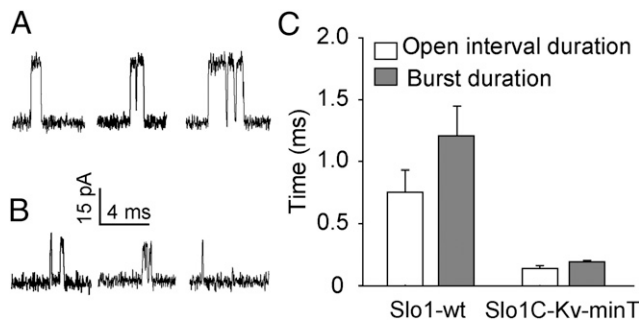
Fig. 6. Open-interval duration, burst duration, and single-channel conductance are reduced in SloC-Kv-minT channels. (*A* and *B*) Single-channel recordings at +80 mV from Slo1-WT channels (*A*) and from Slo1C-Kv-minT channels without the gating ring (*B*). Note reduction of current amplitudes in *B*. (*C*) Bar graphs showing the decrease in mean open-interval and burst duration for Slo1C-Kv-minT channels. Symmetrical 150 mM K$^+$ was used.

for data typically collected from +80 to +140 mV). The ring of negative charge (E321 and E324) at the entrance to the inner cavity that doubles the outward conductance of Slo1-WT channels (32, 33) is retained in the Slo1C-Kv-minT channels, so the reduced conductance does not involve a reduction in the ring of negative charge.

The Gating Ring Is Not Required for Block by External Iberiotoxin and Tetraethylammonium. Because the single-channel conductance was unexpectedly reduced upon replacement of the gating ring with the Kv-minT construct, the possibility arises that other properties of the core pore-gate domain might be altered also. To explore this possibility, we first tested the effect of the highly specific Slo1 channel blocker iberiotoxin (34) on Slo1C-KvT channels. The application of 60 nM iberiotoxin to the external membrane surface of outside-out macropatches (+180 mV) reduced currents $78 \pm 3\%$ ($n = 5$), which was not significantly different from the $82 \pm 3\%$ ($n = 7$, $P = 0.46$) reduction for Slo1-WT channels (Fig. S3*A*). We next tested the effect of external application of the generic K$^+$ channel blocker tetraethylammonium (TEA), because Slo1 channels are known to be highly sensitive to blocking by external TEA (35, 36). We found that 2 mM TEA (+70 mV) reduced Slo1C-KvT whole-cell currents by $81 \pm 2\%$, which was not significantly different from the $85 \pm 4\%$ reduction seen for Slo1-WT currents ($n = 6$, $P = 0.43$) (Fig. S3*B*). Both blocking agents also were tested on Slo1C-Kv-minT with similar effects. Hence, as might be expected, the gating ring is not required for external blocking by iberiotoxin and TEA.

The Gating Ring Is Not Required for β1 Subunits to Slow the Activation of Slo1 Channels. The β subunits are integral membrane proteins with two transmembrane segments that interact with Slo1-WT α subunits and alter various channel properties such as kinetics (37). Although some of the various β subunits may interact with both the core and tail of Slo1-WT channels, the β1 subunit may interact only with the core, slowing the rate of activation of the current (38, 39). Consistent with the previous results, we observed that coexpression of β1 with Slo1-WT produced currents that activated more slowly than those of Slo1-WT α subunits alone (Fig. S3*C*). In a similar manner, coexpression of the β1 subunit with the Slo1C-KvT and Slo1C-Kv-minT constructs also produced currents that activated significantly more slowly than in the absence of the β1 subunits (Fig. S3*C*). In addition, the slow current decrease observed after activation was absent for all three constructs (Slo1-WT, Slo1C-KvT, and Slo1C-Kv-minT) when coexpressed with β1 subunits (Fig. S3*C*). Thus, the gating ring is not required for β1 subunits to interact functionally with Slo1 channels.

Discussion

The Core Can Be Expressed Without the Gating Ring. The fact that Slo1 channels are conserved in invertebrates as well as vertebrates implies that core and tail (Fig. 1) have been associated for more than 500 million years, raising the possibility that core and tail have become so interdependent that the core no longer can function without the tail. Our laboratories and others had tried to express the core without the gating ring but without success. A detailed analysis of truncated Slo1 constructs which failed to express currents indicated difficulties in protein processing, tetramerization, and export from the ER to the plasma membrane (24). We achieved robust expression of Slo1 cores without gating rings by preserving the tetramerization domain of Slo1 (Fig. 1) and either replacing the 827-residue tail that forms the gating ring with the last 74 residues of the Kv1.4 C terminus or attaching a much shorter 11-residue C terminus that included the five-residue motif from KV1.4 for processing and surface expression (25) and also the last three residues of the C terminus of Kv1.4 (Fig. 1).

Functions of the Core and Gating Ring. Our experiments directly show the major functions of the core and gating ring of Slo1 channels. Voltage-dependent gating (Figs. 2–5 and Fig. S2), blocking by iberiotoxin, TEA, and Mg^{2+} (Fig. 4*A* and Fig. S3 *A* and *B*), and slowed activation with β1 subunits (Fig. S3*C*) did not require the gating ring. Hence, these are properties of the core. In contrast, Ca^{2+} and Mg^{2+} activation was not observed in the absence of the gating ring (Figs. 4 and 5, Figs. S1 and S2, and Table S1). Hence, Ca^{2+} and Mg^{2+} activation are conferred by the gating ring through allosteric interactions with the core. These observations confirm previous prognostications (31). It follows from these findings that allosteric interactions of the gating ring with the core are not required for channel opening or closing or for voltage-dependent gating. Hence, the core of Slo1 with attached short tails is sufficient to form a voltage-gated channel. Our observations of no significant Ca^{2+} and Mg^{2+} activation in the absence of the gating ring indicates that no functional Ca^{2+} and Mg^{2+} activation sites are restricted to the core, as is consistent with previous studies showing that mutating sites on the gating ring can eliminate all Ca^{2+} and Mg^{2+} activation (13, 14, 40).

In addition we found that replacing the gating ring with the short tails (*i*) inhibited activation by right-shifting the V$_{1/2}$ to more positive voltages (Fig. 2*C*); (*ii*) greatly decreased mean open-interval duration and burst duration (Fig. 6*C* and Table S2); and (*iii*) decreased the apparent mean single-channel conductance (Fig. 6 *A* and *B*). If these alterations in gating and conductance reflect the baseline properties of the core in the absence of the gating ring, then the right-shift in activation and decreased burst duration could arise if the unliganded gating ring normally applies a passive tension to S6 through the RCK1–S6 linkers to facilitate activation. Consistent with this possibility, decreasing passive tension in the linkers of Slo1-WT by lengthening the RCK1–S6 linkers also right-shifts the activation curve and decreases burst duration (21). The apparent decreased conductance may reflect gating to subconductance levels in the absence of the gating ring. However, at this time we cannot rule out the possibility that the tetramerization domains and appended tails are determinants of these properties. Peptides are known to alter gating of Slo1-WT channels (27). Removal of the gating ring in Slo1-WT channels immediately after the S6 helix without appending tails could resolve this issue, but attempts to express such constructs have not been successful so far (24).

The gating ring has been removed with trypsin digestion from *Methanobacterium thermoautotroficum* (MthK), a prokaryotic Ca^{2+}-dependent K$^+$ channel (41). Like Slo1, MthK has an intracellular gating ring formed by four pairs of RCK1 and RCK2 domains, but with differences in gating ring structure (23, 42, 43).

PHYSIOLOGY

The mean open times and conductance of MthK were little changed by removing its gating ring (41), in contrast to the marked decreases we observed for Slo1 when the gating ring was replaced with short peptide tails. These contrasting results might be related to the fact that, unlike Slo1 channels, the MthK core includes only a pore-gate domain without voltage-sensor domains (43). Thus, MthK is without potential allosteric input from contact between the gating ring and voltage sensor as in Slo1 channels (42). However, we cannot rule out the possibility that the differences might arise from the short peptide tails used to replace the gating ring in Slo1.

Implications for Allosteric Gating. Allosteric models for the gating of Slo1 channels typically assume relatively independent action of Ca^{2+} and voltage to activate the channel (31, 44, 45). Consistent with these models, the channel can be activated without calcium at very high positive membrane potentials (46) or in the presence of high Ca^{2+} over the range of physiological voltages (7–9, 45). The experimental data and models for gating indicate that the core and gating ring interact allosterically, so that Ca^{2+} binding

can move the voltage sensors and, reciprocally, that voltage-sensor movement can change the calcium-binding affinity (31, 40, 45). The allosteric interactions and transduction pathways between gating ring and core involved in these processes still are not well understood. A number of questions regarding these complex interactions now may be pursued with our constructs, because the allosteric interactions might be easier to understand if the properties of the core are defined without the pushes and pulls normally provided by the gating ring.

Materials and Methods

Standard molecular biology methods (12), *Xenopus* oocyte expression systems (12, 13, 47), and electrophysiological techniques (12, 13, 21, 48) were used. The indicated concentrations of Ca^{2+} and Mg^{2+} were applied to the intracellular membrane surface. Experiments were at room temperature. Error estimates are SEM. See *SI Materials and Methods* for more details.

1. Nelson MT, et al. (1995) Relaxation of arterial smooth muscle by calcium sparks. *Science* 270(5236):633–637.
2. Brenner R, et al. (2000) Vasoregulation by the beta1 subunit of the calcium-activated potassium channel. *Nature* 407(6806):870–876.
3. Robitaille R, Garcia ML, Kaczorowski GJ, Charlton MP (1993) Functional colocalization of calcium and calcium-gated potassium channels in control of transmitter release. *Neuron* 11(4):645–655.
4. Montgomery JR, Meredith AL (2012) Genetic activation of BK currents in vivo generates bidirectional effects on neuronal excitability. *Proc Natl Acad Sci USA* 109(46):18997–19002.
5. Fettiplace R, Fuchs PA (1999) Mechanisms of hair cell tuning. *Annu Rev Physiol* 61:809–834.
6. Shao LR, Halvorsrud R, Borg-Graham L, Storm JF (1999) The role of BK-type Ca^{2+}-dependent K^+ channels in spike broadening during repetitive firing in rat hippocampal pyramidal cells. *J Physiol* 521(1)1:135–146.
7. Marty A (1981) Ca-dependent K channels with large unitary conductance in chromaffin cell membranes. *Nature* 291(5815):497–500.
8. Pallotta BS, Magleby KL, Barrett JN (1981) Single channel recordings of Ca^{2+}-activated K^+ currents in rat muscle cell culture. *Nature* 293(5832):471–474.
9. Latorre R, Vergara C, Hidalgo C (1982) Reconstitution in planar lipid bilayers of a Ca^{2+}-dependent K^+ channel from transverse tubule membranes isolated from rabbit skeletal muscle. *Proc Natl Acad Sci USA* 79(3):805–809.
10. Hille B (2001) *Ion Channels of Excitable Membranes* (Sinauer Associates, Inc., Sunderland, MA).
11. Atkinson NS, Robertson GA, Ganetzky B (1991) A component of calcium-activated potassium channels encoded by the Drosophila slo locus. *Science* 253(5019):551–555.
12. Butler A, Tsunoda S, McCobb DP, Wei A, Salkoff L (1993) mSlo, a complex mouse gene encoding "maxi" calcium-activated potassium channels. *Science* 261(5118):221–224.
13. Schreiber M, Salkoff L (1997) A novel calcium-sensing domain in the BK channel. *Biophys J* 73(3):1355–1363.
14. Xia XM, Zeng X, Lingle CJ (2002) Multiple regulatory sites in large-conductance calcium-activated potassium channels. *Nature* 418(6900):880–884.
15. Shi J, et al. (2002) Mechanism of magnesium activation of calcium-activated potassium channels. *Nature* 418(6900):876–880.
16. Hou S, Xu R, Heinemann SH, Hoshi T (2008) Reciprocal regulation of the Ca^{2+} and H^+ sensitivity in the SLO1 BK channel conferred by the RCK1 domain. *Nat Struct Mol Biol* 15(4):403–410.
17. Tang XD, et al. (2003) Haem can bind to and inhibit mammalian calcium-dependent Slo1 BK channels. *Nature* 425(6957):531–535.
18. Hou S, Xu R, Heinemann SH, Hoshi T (2008) The RCK1 high-affinity Ca^{2+} sensor confers carbon monoxide sensitivity to Slo1 BK channels. *Proc Natl Acad Sci USA* 105(10):4039–4043.
19. Schubert R, Nelson MT (2001) Protein kinases: Tuners of the BK_{Ca} channel in smooth muscle. *Trends Pharmacol Sci* 22(10):505–512.
20. Zhang G, Xu R, Heinemann SH, Hoshi T (2006) Cysteine oxidation and rundown of large-conductance Ca^{2+}-dependent K^+ channels. *Biochem Biophys Res Commun* 342(4):1389–1395.
21. Niu X, Qian X, Magleby KL (2004) Linker-gating ring complex as passive spring and Ca^{2+}-dependent machine for a voltage- and Ca^{2+}-activated potassium channel. *Neuron* 42(5):745–756.
22. Lee US, Cui J (2010) BK channel activation: Structural and functional insights. *Trends Neurosci* 33(9):415–423.
23. Yuan P, Leonetti MD, Hsiung YC, MacKinnon R (2012) Open structure of the Ca^{2+} gating ring in the high-conductance Ca^{2+}-activated K^+ channel. *Nature* 481(7379):94–97.
24. Schmalhofer WA, et al. (2005) Role of the C-terminus of the high-conductance calcium-activated potassium channel in channel structure and function. *Biochemistry* 44(30):10135–10144.
25. Li D, Takimoto K, Levitan ES (2000) Surface expression of Kv1 channels is governed by a C-terminal motif. *J Biol Chem* 275(16):11597–11602.
26. Quirk JC, Reinhart PH (2001) Identification of a novel tetramerization domain in large conductance K(ca) channels. *Neuron* 32(1):13–23.
27. Li W, Aldrich RW (2006) State-dependent block of BK channels by synthesized shaker ball peptides. *J Gen Physiol* 128(4):423–441.
28. Díaz L, et al. (1998) Role of the S4 segment in a voltage-dependent calcium-sensitive potassium (hSlo) channel. *J Biol Chem* 273(49):32430–32436.
29. Ma Z, Lou XJ, Horrigan FT (2006) Role of charged residues in the S1-S4 voltage sensor of BK channels. *J Gen Physiol* 127(3):309–328.
30. Savalli N, Pantazis A, Yusifov T, Sigg D, Olcese R (2012) The contribution of RCK domains to human BK channel allosteric activation. *J Biol Chem* 287(26):21741–21750.
31. Hoshi T, Pantazis A, Olcese R (2013) Transduction of voltage and Ca^{2+} signals by Slo1 BK channels. *Physiology (Bethesda)* 28(3):172–189.
32. Brelidze TI, Niu X, Magleby KL (2003) A ring of eight conserved negatively charged amino acids doubles the conductance of BK channels and prevents inward rectification. *Proc Natl Acad Sci USA* 100(15):9017–9022.
33. Nimigean CM, Chappie JS, Miller C (2003) Electrostatic tuning of ion conductance in potassium channels. *Biochemistry* 42(31):9263–9268.
34. Galvez A, et al. (1990) Purification and characterization of a unique, potent, peptidyl probe for the high conductance calcium-activated potassium channel from venom of the scorpion Buthus tamulus. *J Biol Chem* 265(19):11083–11090.
35. Blatz AL, Magleby KL (1984) Ion conductance and selectivity of single calcium-activated potassium channels in cultured rat muscle. *J Gen Physiol* 84(1):1–23.
36. Vergara C, Moczydlowski E, Latorre R (1984) Conduction, blockade and gating in a Ca^{2+}-activated K^+ channel incorporated into planar lipid bilayers. *Biophys J* 45(1):73–76.
37. Contreras GF, Neely A, Alvarez O, Gonzalez C, Latorre R (2012) Modulation of BK channel voltage gating by different auxiliary β subunits. *Proc Natl Acad Sci USA* 109(46):18991–18996.
38. Morrow JP, et al. (2006) Defining the BK channel domains required for beta1-subunit modulation. *Proc Natl Acad Sci USA* 103(13):5096–5101.
39. Liu G, et al. (2010) Location of modulatory beta subunits in BK potassium channels. *J Gen Physiol* 135(5):449–459.
40. Sweet TB, Cox DH (2009) Measuring the influence of the BKCa beta1 subunit on Ca^{2+} binding to the BKCa channel. *J Gen Physiol* 133(2):139–150.
41. Li Y, Berke I, Chen L, Jiang Y (2007) Gating and inward rectifying properties of the MthK K^+ channel with and without the gating ring. *J Gen Physiol* 129(2):109–120.
42. Yuan P, Leonetti MD, Pico AR, Hsiung Y, MacKinnon R (2010) Structure of the human BK channel Ca^{2+}-activation apparatus at 3.0 A resolution. *Science* 329(5988):182–186.
43. Jiang Y, et al. (2002) Crystal structure and mechanism of a calcium-gated potassium channel. *Nature* 417(6888):515–522.
44. Magleby KL (2003) Gating mechanism of BK (Slo1) channels: So near, yet so far. *J Gen Physiol* 121(2):81–96.
45. Horrigan FT (2012) Perspectives on: Conformational coupling in ion channels: Conformational coupling in BK potassium channels. *J Gen Physiol* 140(6):625–634.
46. Horrigan FT, Cui J, Aldrich RW (1999) Allosteric voltage gating of potassium channels I. Mslo ionic currents in the absence of Ca^{2+}. *J Gen Physiol* 114(2):277–304.
47. Zhang Y, Niu X, Brelidze TI, Magleby KL (2006) Ring of negative charge in BK channels facilitates block by intracellular Mg^{2+} and polyamines through electrostatics. *J Gen Physiol* 128(2):185–202.
48. Nimigean CM, Magleby KL (1999) The beta subunit increases the Ca^{2+} sensitivity of large conductance Ca^{2+}-activated potassium channels by retaining the gating in the bursting states. *J Gen Physiol* 113(3):425–440.

Budelli et al.